DRAFT VERSION MARCH 15, 2016
Preprint typeset using LaTeX style AASTeX6 v. 1.0

PHYS 502 MATHEMATICAL PHYSICS II TERM PAPER: CHARACTERIZING THE LONG-TERM VARIABILITY OF 4U 1705-44 EVIDENCE OF AN UNDERLYING NON-LINEAR DOUBLE-WELLED OSCILLATOR

REBECCA PHILLIPSON[1]
Department of Physics, Drexel University
3141 Chestnut St
Philadelphia, PA 19104, USA

ABSTRACT

The low-mass X-ray binary 4U1705-44 exhibits long-term semi-periodic variability with a timescale of several hundred days. The All-Sky Monitor (ASM) aboard the Rossi X-ray Timing Explorer (RXTE) and the Japanese X-ray All-Sky Monitor (MAXI) aboard the International Space Station together have continuously observed the source from December 1995 through the present. The combined ASM-MAXI data provides a continuous time series over fifty times the length of the timescale of interest. The phase space embedding of the flux versus its first derivative shows a strong resemblance to the double-welled nonlinear Duffing oscillator. Topological analysis can help us identify fingerprints in the phase space of a system unique to its equations of motion. If such fingerprints are the same between two systems, then their equations of motion must be closely related. We therefore found a range of parameters for which the Duffing oscillator closely follows the time evolution of 4U1705-44 and from this range chose 6 different numerical Duffing time series. We can extract low-period, unstable periodic orbits from the 4U1705-44 and numerical Duffing time series and compare their topological information in phase space, such as their relative rotation rates. Assigning a logical sequence name to each orbit, the relative rotation rates can be compiled into a unique intertwining matrix. The numerical Duffing time series and the 4U1705-44 intertwining matrices are identical, providing strong evidence that they share the same underlying template. The implications of this equivalence suggests that we can look to the Duffing equation to describe the X-ray binary variability.

Keywords: accretion, accretion disks — stars: individual (4U1705-44) — stars: neutron — X-rays: stars

1. INTRODUCTION

X-ray binaries exhibit periodicities on multiple time scales, which give information about the physical mechanisms at play. High magnetic fields and disc-magnetosphere interactions create pulsations on time scales from milliseconds to seconds. Orbital modulations are seen from minutes to tens of days. A number of X-ray binaries show evidence of long-term periodicities, or superorbital periods, on time-scales much longer than their orbital periods. Some X-ray binaries have variability on time-scales of over a hundred days that are not strictly periodic.[5,6] For the first time, long data sets spanning over a decade are available, providing many cycles to observe this variability. The mechanism driving such variability is not well understood. For low-mass X-ray binaries (LMXBs), it is generally accepted that the accretion is primarily due to a substantial accretion disc, which is unstable to irradiation-driven warping.[7] The precession of the accretion disc is potentially the mechanism underlying the observed long periods. Warped accretion discs are also invoked to explain phenomena observed across many systems including high-mass X-ray binaries, cataclysmic variables, proto-planetary discs and active galactic nuclei.[14] One relevant example is SS433, which has a measured 160-day precession of the relativistic jets identified to be associated with precession of the accretion disc.[19]

In this study, we consider the low-mass X-ray binary, 4U1705-44, which belongs to the class of atoll sources and exhibits the high-amplitude transitions and non-periodic long-term variability of interest.[1,13,9] 4U1705-44 is a neutron star (identified by its Type I bursts) of approximately 1.4 solar masses $(1.1 - 1.6\,M_{sol})$[15] at a distance of $7.4\,kpc$. An infrared counterpart has been observed suggesting a dwarf star companion with a 1-10hr orbital period.[10] The RXTE (Rossi X-ray Timing Explorer) All Sky Monitor obtained approximately 14 years of daily monitoring in the 2-20 keV energy range

of 4U1705-44 with its scan of 80% of the sky every 90 minutes. MAXI (Monitor of All-Sky X-ray Image) onboard the ISS, in operation since August 2009, scans the sky every 96 minutes and continues to provide daily monitoring on 4U1705-44. With MAXI and RXTE combined, we have a 14+ year light curve revealing over 20 cycles of the high amplitude transitions on the order of hundreds of days. The long-term modulations, which have also been observed in other LMXBs, are not strictly periodic. In fact, we propose the long-term variability is reminiscent of a nonlinear double-welled oscillator. After investigations into various oscillators, we purport that the Duffing oscillator is a candidate to describe the system. The parameter ranges that best represent the 4U1705-44 light curve are in the chaotic regime of the Duffing Oscillator. Thus, we use analyses appropriate for non-linear and chaotic time series.

There are two broad approaches to understanding chaotic behavior in dynamical systems. The metric approach generally involves computing the Lyapunov exponents and various dimensions, such as the Correlation and Minkowski dimensions, giving a tight range for the fractal dimension. However, these methods require very large data sets and degrade rapidly with noise. The topological approach, as introduced by Solari & Gilmore (1988),[16,17] involves the identification of the two mechanisms that are responsible for the creation of a strange attractor. These two mechanisms, the stretching and squeezing mechanisms correlating to the sensitive dependence on initial conditions and recurrence phenomenon, respectively, can be characterized by computing how the unstable periodic orbits are uniquely organized. In fact, it is possible to determine how the unstable periodic orbits embedded in the attractor are organized in terms of a set of integers. Extracting these integers from a time series is robust against noise and can be performed for smaller data sets.[12,18,11]

Thus, we will follow the topological approach and calculate the unique set of integers, called the relative rotation rates (RRR), for 4U1705-44 and for the Duffing Oscillator.[17] By extension of the Birman-Williams theorem,[8,23] two chaotic attractors are equivalent if they are described by branched manifolds that can be smoothly deformed, one into the other. In other words, the RRR will remain unchanged under transformations and control-parameter changes. Conversely, the 4U1705-44 and Duffing Oscillator time series share the same underlying template if their RRR are identical. Identifying the underlying template of 4U1705-44 via the RRR allows for the prediction of the RRR of all other possible orbits in the time series and provides a qualitative model for the flow that uniquely generates the chaotic time series. More significantly, if both 4U1705-44 and Duffing Oscillator time series share the same underlying template, then we can look to the Duffing Oscillator equation and its template to make qualitative predictions of the behavior of 4U1705-44 and infer possible physical parameters of the system.

The topological analysis procedure that we use can be summarized as follows. For the 4U1705-44 data, we will determine the lowest order period of an unstable periodic orbit via the Close Returns method as used in Boyd, et. al (1994)[4,11] and via a dynamical power spectra analysis. Using the close returns method and determined lowest order period, we will locate and extract regions in the time series that can be used as surrogates for the unstable periodic orbits. We will then compute the topological invariants of Relative Rotation Rates of all pairs of periodic orbits extracted from the time series and compile these RRR into a matrix. We will then perform a nearly identical analysis on a numerically generated time series from the Duffing Oscillator equations resulting in the Duffing RRR matrix. Finally, we will compare the resulting intertwining matrices followed by a discussion and concluding remarks.[12]

2. DATA AND METHODS

The construction of the 4U1705-44 time series consisted of combining RXTE ASM and MAXI data. We determined the cut-off point of the ASM data to be where the daily measurements consistently exceeded the 3σ range in both the 4U1705-44 data and the same daily monitoring of the Crab nebula, which for our purposes is generally considered to be a reliable and stable reference. MAXI started its observations of 4U1705-44 before this cut-off point and we could therefore use the overlap to appropriately scale the MAXI data to the ASM data. Finally, we normalized the entire combined data set for comparison to the numerically generated Duffing data. The resulting time series and phase-space trajectory are plotted in Fig. 1 and Fig. 2.

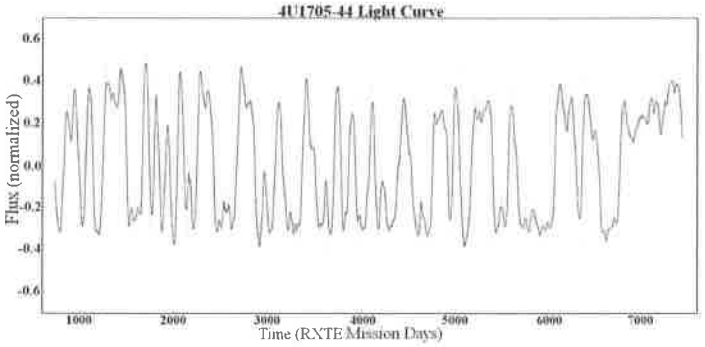

Figure 1. 2-20 keV Flux of 4U1705-44, December 1995 to present, in RXTE Mission Days. The gray curve is the raw light curve and associated error. The green curve was produced by applying a high-pass filter and replacing data points whose errors were more than 5σ or were missing with interpolated points from the surrounding 3 point mean.

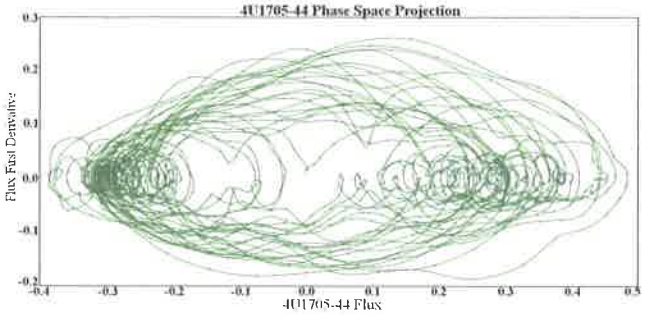

Figure 2. 2-20 keV Flux of 4U1705-44 against its first derivative, over the time period of December 1995 to present. The blue crosses represent the actual data points and the green curve represents a cubic-spline interpolation for smoothness.

A generic form involving five parameters of the Duffing equation was used. That is,

$$\ddot{x} = \delta\dot{x} + \beta x^3 - \alpha x + \gamma \cos \omega t \qquad (1)$$

Solutions were generated on a rolling basis using 4th-order Runge-Kutta within randomly sampled parameter ranges. Those solutions with similar frequency of low-order, low-high amplitude transitions and double-welled phase space features whereby one well was favored over the other predominated an increasingly narrow range in parameter space. These parameters were as follows:

$\alpha = [6.4, 8.2]$, nonlinearity of restoring force
$\beta = [4.6, 7.5]$, stiffness of oscillator
$\delta = [0.25, 0.48]$, size of damping
$\omega = [3.6, 4.5]$, driving frequency
$\gamma = -[5, 7]$, amplitude of forcing

We chose the same time scaling and sampling rate as 4U1705-44 and normalized the numerical data for comparison to the ASM-MAXI data of 4U1705-44. We chose six different representative Duffing solutions with lengths ten times that of the 4U1705-44 data. Portions of the numerical time series and phase-space trajectory of one of these solutions is displayed in Fig. 3 and Fig. 4.

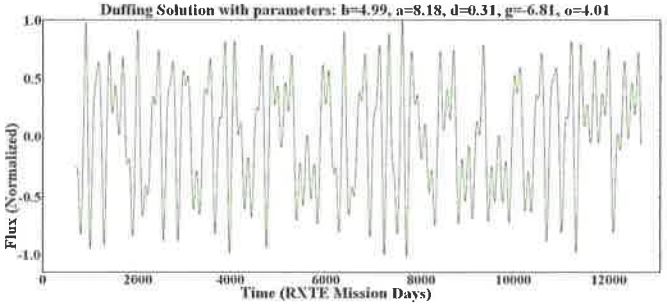

Figure 3. Numerical Flux from Duffing Equation, in RXTE Mission Days. The full time series was produced to be 10 times the length of the 4U1705-44 data set. Only the first sixth of the time series is plotted here.

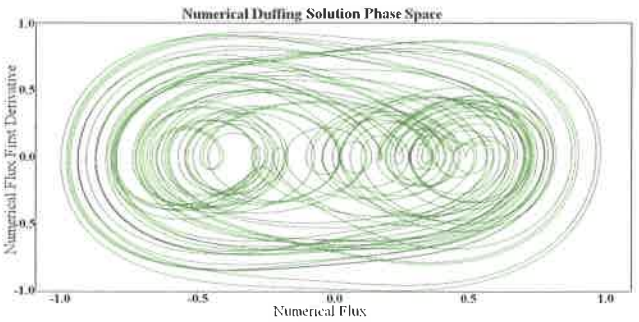

Figure 4. Numerical Flux of Duffing Equation against its first derivative, in RXTE Mission Days.

3. FINDING THE LOWEST ORDER PERIOD OF 4U1705-44

Since the driving period for 4U1705-44 is unknown, we use the method of close returns[4,11], ideal for small, chaotic data sets to identify nearly closed orbits near unstable periodic orbits of low period. Fig. 5 shows the close returns plot of i vs. p locating these segments. A blue point is plotted at (i, p) when, for that time i, there is a point p days later that is close (we determined within 10% of the max as "close") to the value at time i. Regions of the time series that are close to repeating itself appear as short horizontal lines. These correlate to sections in the light curve in which the time series comes close enough to an unstable periodic orbit such that it remains close for at least one period. We extract all such regions from the light curve and find these lowest order orbits have periods between 110 and 200 days.

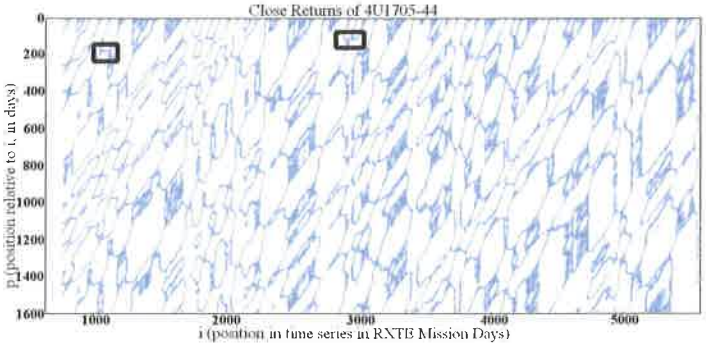

Figure 5. A blue point is plotted at (i, p) when, for that time i, there is a point p days later that is close to the value at time i. The color intensity of a point corresponds directly to its closeness to the starting point. Regions of the time series that are close to repeating itself appear as short horizontal lines, two examples of which are highlighted.

We can corroborate the lowest order period obtained from the close returns analysis with the dynamic power spectrum. Fig. 6 shows the total power spectra of the raw light curve of 4U1705-44 plotted against the period in the left pane. All of the significant power in the spectrum is at longer periods, corresponding to low fre-

quencies, indicative of long-term variability. The right pane is the dynamic power spectrum showing the power spectrum of a window size of 4096 days as it evolves over time. The ends are padded with randomized noise. The lowest order period varies between 130 and 170 days. We also see distinct evidence for the appearance of modes of higher order periods.

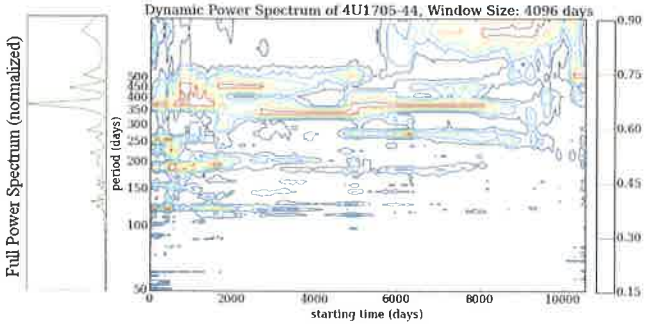

Figure 6. Dynamic Power Spectrum of 4U1705-44, taken with a window size of 4096 days and padding the ends of the data set with numerically generated noise about the mean.

Lastly, for final verification, we analyzed the zero-crossings of 4U1705-44 in order to identify the variation in periodicity. That is, we calculated all the times and corresponding derivatives in which the mean-subtracted light curve crossed zero, distinguishing between an upwards trajectory (up-crossing) and a downwards trajectory (down-crossing). This gave us the amount of time spent in each region of phase space. Time spent below zero (in a low-state of the light curve) corresponds to the left-well seen in phase space; similarly, time spent in the positive, high-state, corresponds to the right-well in phase space. The average period spent in a well is 250 ± 130 days and 58% of the time spent in the left (lower) well. Although the error in the average period is large, this is consistent with there being several tiers of typical periods, as seen in Fig. 7, across this entire range as also evidenced by the dynamical power spectrum.

4. EXTRACTING UNSTABLE PERIODIC ORBITS

We have determined a range for the lowest-order period in the 4U1705-44 data. We have also produced numerical data of the Duffing Oscillator. Its lowest order period is simply the driving period, ω, from the equation, which we know to be 140 days. Starting with the numerically generated Duffing time series, we can easily subtract low-order, unstable periodic orbits from the time series by using a modified version of the close returns method. That is, rather than comparing each position in the time series to every other position ahead, we can choose a period of 140 days and compare each position in the time series to each successive period later, calculate the relative distance and, if this distance falls

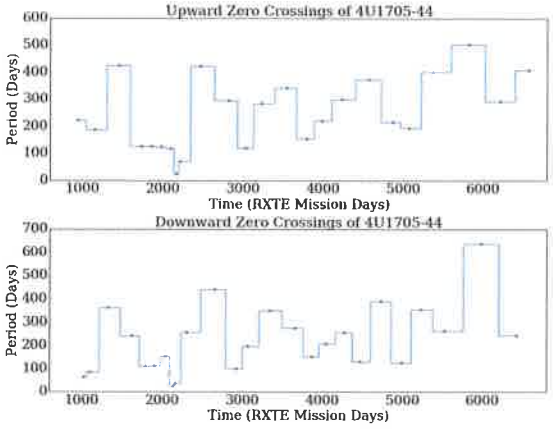

Figure 7. Zero-crossings of 4U1705-44: the upper pane is of successive up-crossings, the lower pane of successive down-crossings.

within a small value, ϵ, and evolves within that neighborhood for at least one period, then we have located an unstable periodic orbit.[11] Such a determination is exemplified in Fig. 8a for the entire time series for a period-1 orbit. Fig. 8b expands a section in which the distance is minimal (e.g. within 10% of the maximum) for an extended amount of time, thus providing us a good candidate for a period-1 orbit.

Using the method of close returns on the numerically generated Duffing solutions, we were able to extract unstable periodic orbits up to period-6 by varying the parameter n in Fig. 8. That is, we were able to locate and extract 5 period-1, 4 period-2, 3 period-3, 4 period-4, 2 period-5 and 2 period-6 orbits.

Given that we determined the lowest order period in the 4U1705-44 data to be in the (narrower) range of 130 to 170 days, we chose the Duffing period-1 length of 140 days for optimal comparison. Using the same method, we thereby reduced the close returns plot in Fig. 5 to a one dimensional version as done in the Duffing case. As a result, we located regions of unstable periodic orbits and successfully extracted three orbits for each period-1, -2 and -3.

5. RELATIVE ROTATION RATES

A strange attracter can be characterized by the invariants that it possesses. The traditional classification of a strange attractor is by the determination of its dynamical and metric invariants, e.g. the Lyapunov exponents and various dimensions (e.g. Correlation or Minkowski). The third type of invariant is topological. Where the first two types are invariant only under coordinate transformations, the topological type is also invariant under control-parameter changes. For experimental conditions in which the control parameters experience perturbations the determination of the topological invariants is appropriate.[16]

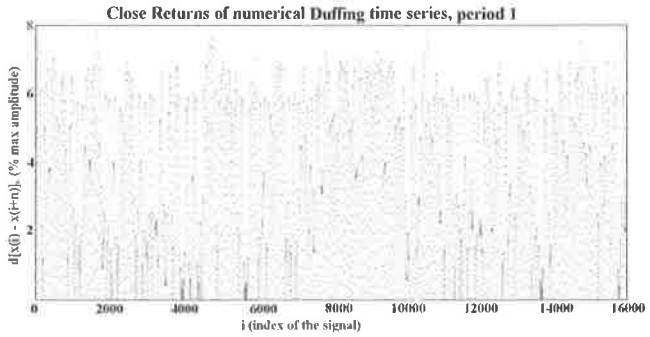

(a)

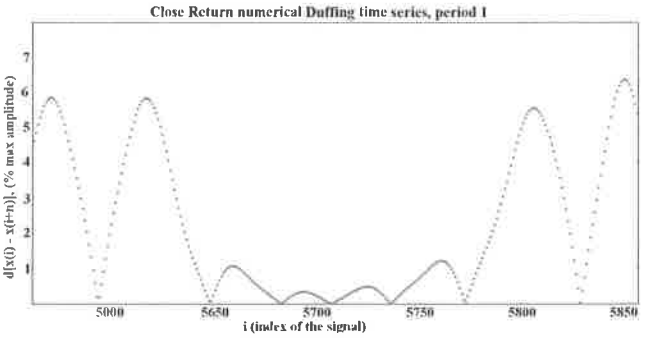

(b)

Figure 8. Relative distances between a point x(i) and x(i+n), $d[x(i) - x(i+n)]$, plotted as a function of i, for a fixed period n. In this example, we are searching for period-1 orbits, which are of length 140 days; (a) is of the full time series, (b) is of the segment about 5700 days.

Topological invariants draw dependence on the periodic orbits existing in a strange attractor. The mechanisms that drive the behavior of a strange attractor uniquely organize all the unstable periodic orbits embedded in that strange attractor. The "stretching" mechanism is correlated to the sensitivity to initial conditions: nearby points essentially repel each other at an exponential rate. However, in order for these two points to not end up at two ends of an infinite spectrum there exists a mechanism that keeps the entire system bounded in phase space such that these two points reach a maximum separation. This latter behavior is associated with the "squeezing" mechanism. Identifying the organization of the unstable periodic orbits can be used to identify these underlying mechanisms and thereby provide us with the "fingerprints" on which the attractor is built. That is, the underlying structure described by these mechanisms is completely responsible for the organization of all periodic orbits in the flow. We are therefore provided with predictive capabilities describing the qualitative and geometric behavior of the attractor.[12]

One of the topological invariants introduced by Solari and Gilmore, 1988,[17] intended to describe periodically driven two-dimensional dynamical systems, such as nonlinear oscillators, is called the Relative Rotation Rates (RRR). When a strange attractor has a "hole" in the middle, as depicted by the Duffing Oscillator and the 4U1705-44 phase space, RRRs can be determined for such systems. Generally speaking, RRRs describe how one periodic orbit rotates around another; or, more specifically, the average value, per period, of this rotation rate.

The relative rotation rates can be computed only after the orbits have been embedded in $\mathbb{R}^3$.[8] We chose a differential phase space embedding[11]:

$$\begin{aligned} x(i) \to y(i) &= \{x(i), dx(i)/dt, d^2x(i)/dt^2\} \\ &\approx \{x(i),\ x(i+1) - x(i-1), \\ &\quad x(i+1) - 2x(i) + x(i-1)\} \end{aligned} \tag{2}$$

Let A be an orbit of period p_A which has intersections $(a_1, a_2, \ldots, a_{p_A})$ with a Poincaré section $t = const$, and similarly for orbit B. The relative rotation rate $R_{ij}(A, B)$ of A around B is defined as:

$$R_{ij}(A,B) = \frac{1}{2\pi p_A p_B} \oint \frac{\boldsymbol{n} \cdot (\boldsymbol{\Delta r} \times d\boldsymbol{\Delta r})}{\boldsymbol{\Delta r} \cdot \boldsymbol{\Delta r}} \tag{3}$$

in which we have defined $\boldsymbol{\Delta r} = [x_B(t) - x_A(t), y_B(t) - y_A(t)]$ is the difference vector between points on the two orbits, $\boldsymbol{n}$ is the unit vector orthogonal to the plane spanned by $\boldsymbol{\Delta r}$ and $d\boldsymbol{\Delta r}$, and the integral extends over $p_A \times p_B$ periods. The initial conditions are the points a_i, b_j on the Poincaré section. All of the relative rotation rates for a system can be assembled into a table, or "intertwining matrix."[16]

An example of the computation of a RRR for a period-4 orbit against another period-4 orbit in the numerical Duffing time series is plotted in Fig. 9. We located the intersection of each extracted periodic orbit with a Poincaré section. Next, we connected each pair of points in the two orbits by a directed line segment. This line segment will evolve in time under the flow and will have undergone an integer number of full rotations (2π radians) in the plane perpendicular to the flow in $p_A \times p_B$ periods. The relative rotation rates can be computed in four equivalent ways.[16] The first is as is defined in Eq. 2. A second, which is most convenient to show graphically, is as follows: Whenever $\Delta r^2 = 0$ and $\Delta r^1 \geq 0$, define $\sigma(t)$:

$$\sigma(t) = \begin{cases} +1 & d\Delta r^2/dt > 0 \\ -1 & d\Delta r^2/dt < 0 \end{cases} \tag{4}$$

Then

$$R_{ij}(A,B) = \frac{1}{p_A p_B} \sum_{0 \leq t \leq T_{p_A p_B}} \sigma(t) \tag{5}$$

Fig. 9(b) shows each time the difference Δr crosses the half line $\Delta r^2 = 0$, $\Delta r^1 > 0$, whereby the crossing

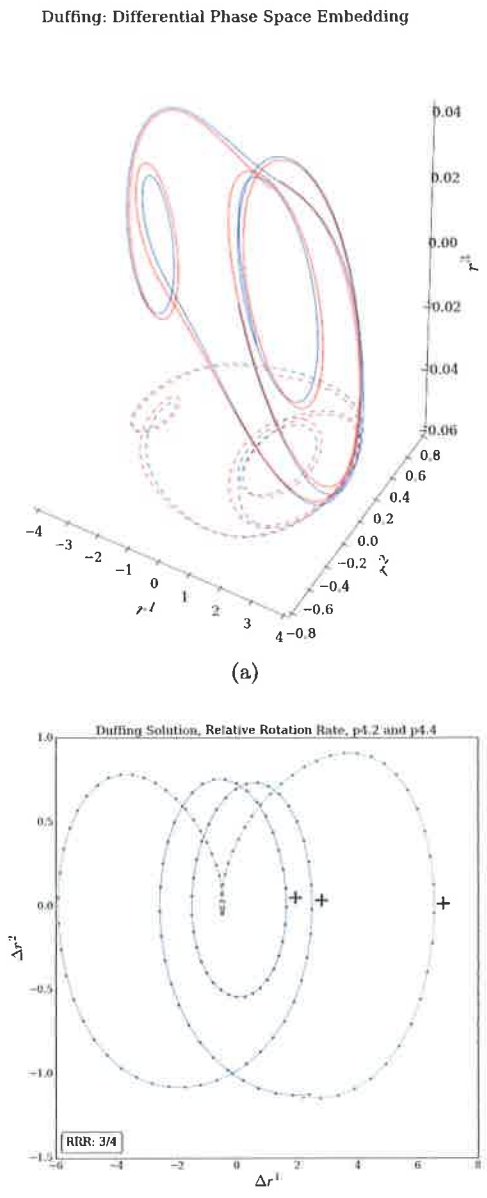

(a)

(b)

Figure 9. Computation of RRR for two period-4 orbits. (a) 3D phase space embedding and projection of a pair of extracted unstable periodic orbits of period 4 from the numerical Duffing solutions over a period $4T$ (just p_A), (b) each time the difference Δr crosses the half line $\Delta r^2 = 0$, $\Delta r^1 > 0$, the crossing direction is counted positive ($\sigma = +1$) if $d\Delta r^2/dt > 0$ and negative if $d\Delta r^2/dt < 0$. Note: the plot shows this done over a period of 4T (rather than $p_A \times p_B$).

direction is counted positive ($\sigma = +1$) if $d\Delta r^2/dt > 0$ and negative if $d\Delta r^2/dt < 0$. For the period-4 compared against a different period-4, we find the RRR is 3/4.

Following the same procedure through with all extracted unstable periodic orbits, we collect the RRRs for both 4U1705-44 and the numerically generated Duffing time series into their respective intertwining matrices. Up through period-3 (the longest period extracted from the 4U1705-44 data) the matrices are identical. If we can eventually extract a period-4, -5, or -6 orbit from the 4U1705-44 data, we will then be able to compare against the full (including all extracted periodic orbits) Duffing intertwining matrix for verification. To reiterate, an intertwining matrix may be associated with any periodic flow. Different flows with the same map may have closely related intertwining matrices. If the matrices are identical the flows may be equivalent. Given that these matrices are identical, it is therefore possible that the flows are equivalent. As such, if the RRRs do agree, then the underlying template of the Duffing oscillator can serve as a geometric model for the dynamics which generate the chaotic time series of the 4U1705-44 system, i.e. the stretching and squeezing mechanisms and the qualitative behaviors they infer for all future periodic orbits.

4U1705-44 Relative Rotation Rates							
	1.1	1.1	1.3	2.1	2.2	3.1	3.2
	$x\gamma$	$x\gamma$	$x\gamma$	$yy\alpha$	$yy\beta$	$xyx\alpha$	$xyx\beta$
1.1	0	1	1	1	1	2/3	2/3
1.2		0	1	1	1	2/3	2/3
1.3			0	1	1	2/3	2/3
2.1				0	1/2		
2.2					0		
3.1						0	2/3
3.2							0

Table 1. Orbits are labeled as (p.n), i.e. the n^{th} orbit of period p; x and y signify the orbit's presence in each lower- or upper- well, γ signifies symmetric orbits, and α, β asymmetric orbits. Only distinct orbits are included in the matrix.

Duffing Relative Rotation Rates									
	1.1	1.1	1.5	2.1	2.2	3.1	3.2	5.1	5.2
	$x\gamma$	$x\gamma$	$x\gamma$	$yy\alpha$	$yy\beta$	$xyx\alpha$	$xyx\beta$		
1.1	0	1	1	1	1	2/3	2/3		
1.2		0	1	1	1	2/3	2/3		
1.5			0	1	1	2/3	2/3		
2.1				0	1/2	2/3	2/3	4/5	4/5
2.2					0	2/3	2/3	4/5	4/5
3.1						0	2/3	2/3	2/3
3.2							0	2/3	2/3
5.1								0	2/5
5.2									0

Table 2. RRRs of numerically generated Duffing time series with the same identifying naming convention of orbits as 4U1705-44 RRRs. Orbits of the same type as in 4U1705-44 are included here, as well as period-5 for illustration.

6. CONCLUSIONS

Exploring the time series of X-ray binary 4U1705-44 is critical to the study of all X-ray binaries because they all share many of the same global characteristics in their high-amplitude transitions and non-periodic variability over the long-term. The mechanism behind this variability is not well understood. A non-linear oscillator is a strong candidate to describe these systems. We have found striking results that beg further analysis: the low-order driving period is between 130 and 170 days, which is seen and highlighted in the power spectra, zero-crossings and close returns analysis of 4U1705-44. Furthermore, the driving frequency (ω) of all six Duffing solutions tend to converge to a range of $3.6 - 4.5$, corresponding to driving periods in the range of 140 to 175 days. The relative rotation rates analysis strongly suggests that 4U1705-44 and the Duffing equation share the same underlying template. The next step in our analysis is to complete the intertwining matrices, obtain additional verification by computing the linking numbers, which is closely related to the relative rotation rates, and computing the intertwining matrices and linking numbers for the other five numerically generated Duffing time series as well as from other external computations of the Duffing oscillator.[18] This all would serve to verify the template identification of 4U1705-44. Lastly, it would also be prudent to compare against other dynamical systems. Already, the intertwining matrix for another chaotic system, the Belousov-Zhabotinsky reaction,[11] is not identical to 4U1705-44 and differs by a non-integer (thus, we can predict that the flows are inequivalent). We will next consider what could be occurring in the 4U1705-44 binary system physically that creates such a strong relationship to the Duffing equation. For example, the long-term driving period could be related to an irradiaion-driven warped accretion disk that precesses over the long-term of over 100s of days. Other possibilities, such as precession of the neutron star spin axis, or a bi-stability in the accretion disk warping modes will also be investigated.[7,14]

Facilities: RXTE(ASM)

Software: Python

REFERENCES

[1]Barret, D., & Olive, J. F. 2002, ApJ, 576, 391-401
[2]Birman, J. S., & Williams, R. F. 1983, Topology, 22, 47-82
[3]Birman, J. S., & Williams, R. F. 1983, Topology, 20, 1-60
[4]Boyd, P. T., Mindlin, G. B., Gilmore, R., Solari, H. G. 1994, ApJ, 431, 425-431
[5]Clarkson, W. I., Charles, P. A., Coe, M. J., Laycock, S., Tout, M. D., Wilson, C. D. 2003, MNRAS, 339, 447-454
[6]Clarkson, W. I., CHarles, P. A., Coe, M. J., Laycock, S. 2003, MNRAS, 343, 1213-1223
[7]Foulkes, S. B., Haswell, C. A., Murray, J. R. 2010, MNRAS, 401, 1275-1289
[8]Gilmore, R. 1998, Rev. of Modern Phys., 70, 4
[9]Hasinger, G., van der Klis, M. 1989, Astron. Astrophys., 225, 79-96
[10]Homan, J., Kaplan, D. L., Van Den Berg, M., Young, A. J. 2009, ApJ, 692, 73-80
[11]Mindlin, G. B., Gilmore, R. 1992, Physica D, 58, 229-242
[12]Mindlin, G. B., Hou, X. J., Solari, H. G., Gilmore, R., Tufillaro, N. B. 1990, Phys. Rev. Lett., 64, 20
[13]Muno, M. P., Remillard, R. A., Chakrabarty, D. 2002, ApJ, 568, 35-39
[14]Ogilvie, G. I., Dubus, G. 2001, MNRAS, 320, 485-503
[15]Olive, J. F., Barret, D., Gierlinski, M. 2003, ApJ, 583, 416-423
[16]Solari, H. G., Gilmore, R., 1988, Phys. Rev. A, 37, 8
[17]Solari, H. G., Gilmore, R., 1988, Phys. Rev. A, 38, 3
[18]Tufillaro, N. B., Solari, H. G., Gilmore, R. 1990, Phys. Rev. A, 41, 10
[19]Whitmire, D. P., & Matese, J. J. 1980, MNRAS, 193, 707-712